Enhancing the Opto-electronic Performance of Thin-film Solar Cells Using Embedded Nanorods Comprised of Single Walled Carbon Nanotubes

Tazrian Noor[1], Md. Hasibul Hossain[1], Ananya Pramanik[1], Asif Al Suny[1], Rifat Bin Sultan[1], Samina Tohfa[1], and Mustafa Habib Chowdhury[1*]

[1]Department of Electrical and Electronic Engineering, Independent University, Bangladesh, Dhaka, Bangladesh

Email: tazriannoor1@gmail.com, hhossain15700@gmail.com, ananya.pramanik55@gmail.com, asif.al.suny@gmail.com, rifatbinsultan2@gmail.com, saminatohfa1@gmail.com, mchowdhury@iub.edu.bd*

Abstract—This computational study uses the Finite-Difference Time Domain (FDTD) method to investigate the opto-electronic performance of amorphous silicon thin-film solar cells (Si TFSCs) that are embedded with arrays of periodic nanorods composed of randomly-oriented single-walled carbon nanotubes (SWCNTs). The diameter of the nanorods were varied between 20 nm-70 nm, and for each diameter, the side-to-side distances between neighboring nanorods (pitch) were varied from 5 nm-30 nm, keeping the nanorod height equal to the absorber layer thickness (550 nm). The optimal short circuit current density obtained was 32.13 mA/cm^2 for a nanorod diameter of 30 nm and pitch of 5 nm, yielding a 351% increase compared to bare Si TFSCs 7.12 mA/cm^2. Additionally, the efficiency increased from 1.62% for bare Si TFSCs to 8.50% for the embedded SWCNT nanorod structure. This study shows the immense potential of using novel carbon-based nanostructures to significantly enhance the optoelectronic performance of solar cells, as well as contributes towards sustainable technology substituting fossil fuels to minimize global warming.

Keywords—Solar cell, Thin-film solar cell, Finite-difference time-domain, FDTD, Plasmonics, Nanorods, Carbon nanotubes, SWCNT, Graphene, Nanostructures, Renewable energy, Sustainable energy.

I. Introduction

The demand for power is ever increasing as the benefits of modern industrial economic growth has brought about a population boom across the world. Fossil fuels, that are the main source of energy, are still providing the majority of the energy requirement of the world. This is unfortunately creating a significant adverse impact on the earth's environment via global warming. Hence, there is a dire need for the widespread deployment of different kinds of renewable energy technologies to mitigate the effects of global warming. As solar energy is abundant, it can be harnessed to decrease the reliance on non-renewable energy sources by providing "green" renewable and sustainable energy. Overall development of solar cells will eventually lead to a sustainable energy and technology in the long run. Commercially available first generation photovoltaic solar cells manufactured from monocrystalline silicon are a hurdle against spread of photovoltaics as they tend to be expensive because they are spliced out of wafers which accounts for 40% production cost and there is loss of refined silicon while cutting [1]. One way to reduce cost is to move to amorphous silicon which is less expensive and abundant than crystalline silicon and secondly reduce the thickness to the scale of micrometer or nanometer level, i.e., move on to second generation thin film solar cells (TFSCs). TFSCs are light-weight due to reduction of absorber material, and a plethora of mobile electronic devices like smart watch, fitness tracker, could use and leverage TFSCs to meet their power needs [2].

But reduction of absorber material significantly reduces the absorption capability of light in the absorber layer of the solar cell and also leads to greater surface recombination [3]. Hence, a number of light-trapping techniques have been used to enhance the light absorption ability of Si TFSCs. It has been shown that plasmonic nanoparticles, nano-grating, and surface textures can significantly enhance the opto-electronic performance of solar cells [4] [5]. Silicon has an absorption window in the 300 nm to 1100 nm region of the solar spectrum, but the reduction of thickness of Si in TFSCs leads to reduced light absorption ability in the visible and near infrared regions [6]. To tackle this problem, this study investigates how single wall carbon nanotubes (SWCNTs) can be used to enhance the optoelectronic performance of Si TFSCs. SWCNTs have a wide range of direct bandgaps, therefore yielding broadband absorption across the solar spectrum [7]. Additionally, SWCNT films have found to have significant charge carrier mobilities even at low intensity light [8]. This is extremely important and can be leveraged to reduce surface recombination in amorphous Si. Subsequently, SWCNTs are known to have good hole carrier capabilities and SWCNT films have been found to have formed heterojunctions leading to greater ease of transporting charges to the electrode [9]. SWCNT films have also been shown to exhibit broadband and tunable plasmonic affects [10]. Previous studies have shown that SWCNTs and SWCNT films were used on top as well as embedded inside different TFSCs to yield desirable

performances [11] [12]. SWCNT have shown to yield better electrical output when placed as a buffer layer between the active layer and cathode in fabricated polymer solar cells [11]. Additionally, polymer hetero-structures experience improved performance when CNTs are placed inside the polymer active layer which leads to greater charge generation [12]. Also, CNTs are not only used in solar cells, but can also be embedded inside transistors to fabricate SWCNT film-based bendable circuit for modern electronic devices, and much more [13]. SWCNTs have also been embedded in perovskite solar cells to make foldable solar cells that also lead to increased performance levels of such solar cells [14]. Previously, dye-sensitized solar cells have been reported to use vertically aligned CNTs, but it faced fabrication hurdles while removing the catalyst and transferring vertically aligned carbon nanotubes to target substrate [15] [16]. Because SWCNT carbon nanotubes films have been widely embedded in different kind of semiconductor materials in various applications, this study explored computationally the possibility of embedding SWCNT-based nanorodshaped structures inside the Si absorbing layer to optimize the optoelectronic performance of Si TFSCs. Additionally, the findings will help towards development of light-weight solar cells which would generate equivalent power but would require a smaller area and material compared to traditional solar cells. Also, there lies the prospect of integrating these light-weight solar cells into smartphones, smart watches, calculators, and other similar small-scale electronic devices.

II. Material and Methods

A. Simulation Setup

The commercial-grade software Ansys Lumerical FDTD Solutions and CHARGE have been used to conduct the necessary simulations presented in this study [17]. The FDTD solver has been used to generate the optical generation rate, which was then imported in CHARGE to calculate the electrical performance parameters.

Fig. 1 shows the 3-D schematic of the simulation setup to perform the optical FDTD simulations in FDTD. The substrate is made of 550 nm thick amorphous Si, with an array of SWCNT-based nanorods of the same height embedded inside the light-absorbing Si layer. The material data used for

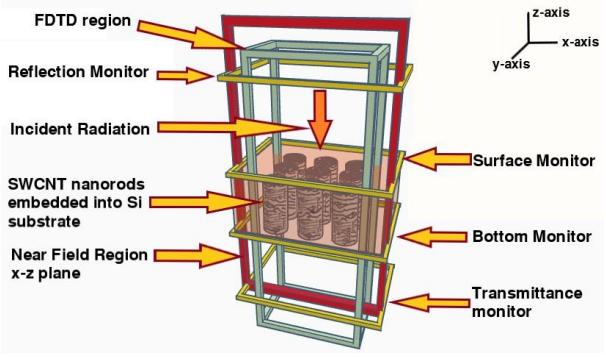

Fig. 1: Schematic showing three-dimensional (3-D) visualization of FDTD simulation setup of embedded SWCNT nanorods inside the light absorbing substrate of a Si TFSC. the carbon nanorods were the broadband constants obtained from aerosol CVD SWCNTs in the spectral range 250-3300 nm by Ermolaev et al [18]. The simulation conditions were as follows: temperature of 300 K, source with solar spectral irradiance of AM 1.5G (plane wave) and intensity of 1000 W/m^2 [19]. Two 2-D frequency domain power monitors along the x-y plane were placed to calculate the power absorption by the substrate - one along the top of the substrate, and the other along the bottom. Two more 2-D power monitors were placed above and below the substrate to calculate the reflectance and transmittance of the substrate. Data from these two monitors were then used to calculate the absorption spectra for bare Si TFSC and substrate with embedded SWCNT nanorods. Finally, in order to observe the near-field enhancement, a power monitor is placed along the x-z plane.

Fig. 2 shows the 3-D schematic of the simulation setup to perform the electrical simulations in the CHARGE solver and in turn obtain the required electrical performance parameter values by importing the optical generation data from the FDTD solver. The front and back contacts are made of Aluminium (Al), and the Si substrate has *p*-type and *n*-type doping concentrations of 10^{16} cm^{-3} and 10^{15} cm^{-3} respectively. The substrate and back contact were extended along the x-axis to ensure the electron-hole pairs are collected properly.

B. Procedure

The investigation involved varying the diameter of the nanorods and the pitch size (distance between adjacent nanorods) for each nanorod diameter, for which the FDTD simulation region was adjusted accordingly as shown in Fig. 3. The diameter of the nanorods were varied 20 nm to 70 nm (at an increment of 10 nm) and the pitch size (side-side distance of neighboring nanorods in the array) was varied from 5 nm to 30 nm (at an increment of 5 nm). Incident radiation of 4001100 nm wavelength was used to match the absorption band of the silicon substrate in the solar spectrum [6]. The optical and electrical parameters calculated are as reported previously [4] [20].

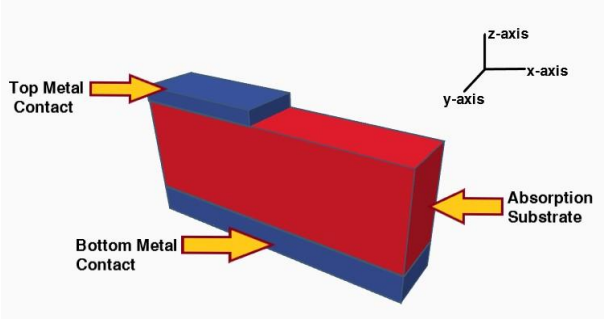

Fig. 2: Schematic showing three-dimensional (3-D) visualization of CHARGE simulation setup of embedded

SWCNT nanorod inside the Si light absorbing to study electrical performance parameters of solar cells.

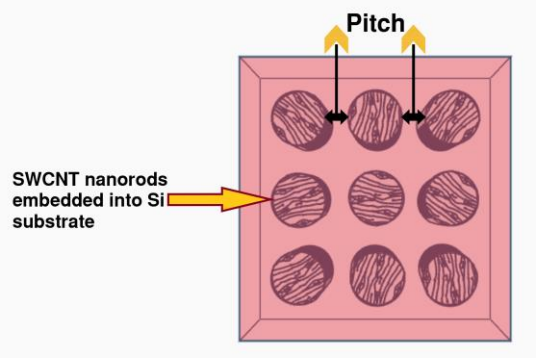

Fig. 3: Top view schematic indicating the side-to-side distance or pitch between nanorods in an array.

- Optical Absorption Factor (g) - This is representative of the amount of light absorbed by the silicon substrate with embedded SWCNT and bare Si TFSCs.
- Short-circuit current density (J_{SC}) - It is the maximum possible current generated per unit area of the solar cell when it is short-circuited (i.e., voltage is zero).
- Open circuit voltage (V_{OC}) - It is the maximum possible voltage that can be generated by a solar cell in opencircuit condition (i.e., current is zero).
- Fill factor (FF) - It is the ratio of the of the maximum possible power output of a solar cell to the product of J_{SC} and V_{OC}.
- Maximum power (P_{max}) - It is the maximum possible power output of the solar cell per unit area.
- Efficiency (η) - It is the percentage of the incident power from the sun that is obtained as electrical output.

The equations mentioned previously can be used to calculate the performance parameters above [4] [19] [20]. Alongside, in order to investigate and comprehend the behavior of the proposed design, optical near-field enhancement images were generated to observe the electromagnetic field distribution in the surrounding area of the SWCNT nanorods as described previously [4] [20].

III. Results and Discussions

A. Comparison of SWCNT modified Si TFSC with Bare Si TFSC

1) Optical Absorption Spectra Analysis: Fig. 4 shows the wavelength-resolved optical absorption spectra of a bare Si TFSC and the optimal configuration of SWCNT nanorods embedded in a Si TFSC. Amorphous silicon has a poor absorption coefficient due to reduced thickness and poor absorption capability across the solar spectrum, especially in the longer near-infrared (NIR) region. The bare Si (red curve) clearly shows that Si has better absorption at shorter wavelengths and percentage absorption gradually declines as the wavelength of incoming photons increases. The optimal configuration of SWCNT nanorods embedded in a Si TFSC (blue curve) significantly boosts the optical absorption capability of the TFSC across all wavelengths. It is interesting to note that

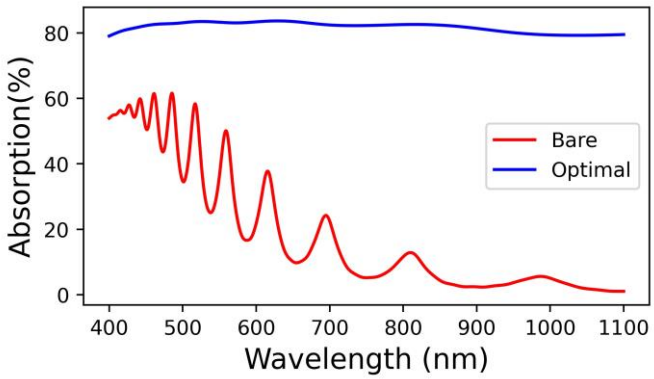

Fig. 4: Percentage absorption of light in a bare Si TFSC (red curve) and the optimal configuration of SWCNT nanorods embedded in a Si TFSC (blue curve).

the percentage optical absorption is approximately constant across the absorption window for the embedded SWCNT case and shows considerable improvement when compared to the bare Si TFSC case at each wavelength point. This broadband enhancement can be attributed to the availability of multiple direct bandgaps in SWCNT which leads to more photon absorption in the solar spectrum [21]. It is well known that light striking graphene (which makes up the SWCNT nanostructure) is trapped and transformed into an ultraslow surface wave. These waves get ”stuck” in graphene and stay there until they are absorbed. The enhanced light absorption by the graphene leads to larger photo-signals which can then generate larger electrical signals [21].

2) Short Circuit Current Density (J_{SC}) Analysis: The amount of free electron-hole pairs generated due to the interaction of incident photons on the solar cell substrate can be depicted from the short circuit current density (J_{SC}) [19]. Fig. 5 pictorially shows the change in J_{SC} as the pitch and diameter

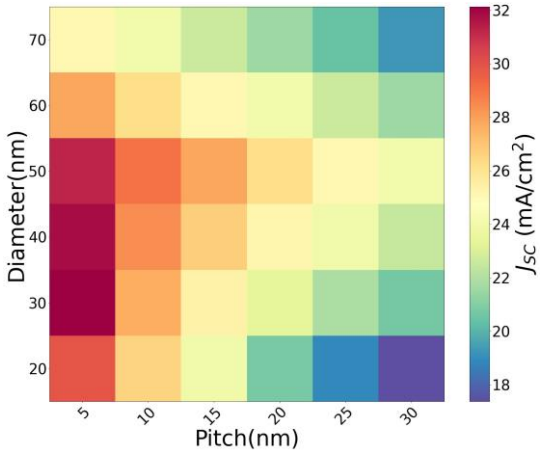

Fig. 5: Variations in short-circuit current density (J_{SC}) with respect to diameter and pitch of SWCNT nanorods embedded in a Si thin-film solar cell.

of the embedded SWCNT nanorods in the Si absorbing layer of the TFSC are varied. The maximum J_{SC} obtained is 32.13 mA/cm^2, for an array of 30 nm diameter nanorods with 5 nm pitch size, compared to J_{SC} of 7.12 mA/cm^2 from the bare Si TFSC (i.e., with no SWCNT modifications). The enhancement might be occurring due to the SWCNTs allowing more efficient electron transport [22]. If the pitch is increased to 10, 15, 20, 25, and 30 nm, while keeping the diameter of the nanorod constant at 30 nm, the J_{SC} values obtained are 27.64, 25.34, 23.36, 21.84, and 20.68 mA/cm^2 respectively. This shows a decreasing trend in J_{SC} as the pitch size increases, since there are now fewer number of SWCNT per unit area.

3) Open Circuit Voltage (V_{OC}) Analysis: Unlike J_{SC}, the change in V_{OC} is not significant, demonstrated in Fig. 6. Here, the optimized embedded SWCNT nanorods holds the highest V_{OC} which is 0.359 V while the bare Si substrate has a V_{OC} of 0.314 V. Gradual increase in V_{OC} is seen up to 50 nm nanorod diameter and for pitch size constant at 5 nm and the lowest V_{OC} found is for 30 nm pitch size and 20 nm nanorod diameter (note the purple colored-block on the lower right corner in Fig. 6). Nevertheless, improved performance in V_{OC} can be observed for all pitch sizes at different diameters when compared to bare Si substrate (0.314 V).

4) Fill Factor (FF) Analysis: Fill Factor is an indication of the solar cell's quality. Fig. 7 shows a similar trend in change in fill factor as discussed earlier analyzing other performance parameters, with a maximum fill factor of 0.7378 obtained for 50 nm diameter nanorods with pitch size of 5 nm. However, there is minor enhancement similar to V_{OC} since the FF for bare Si substrate is found to be 0.7256. It can also be found that some of the SWCNT configurations have a lower FF compared to the bare Si substrate (0.7256).

5) Maximum Output Power (P_{max}) Analysis: The maximum output power (P_{max}) that can be practically obtained from a solar cell determines how well it can convert incident photons to useful energy. Fig. 8 shows the change in P_{max}, with the optimal value of 8.504 mW/cm^2 coming from nanorods of 30

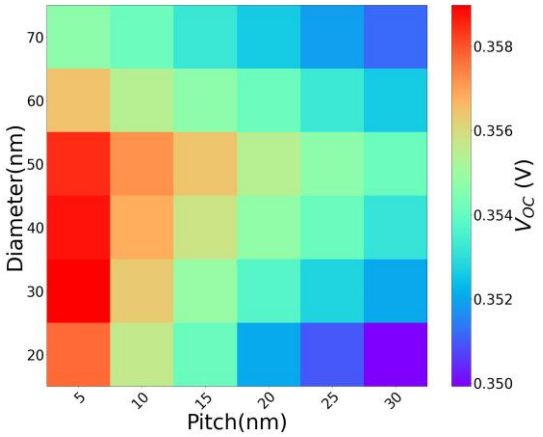

Fig. 6: Variations in open-circuit voltage (V_{OC}) with respect to diameter and pitch of SWCNT nanorods embedded in a Si thin-film solar cell.

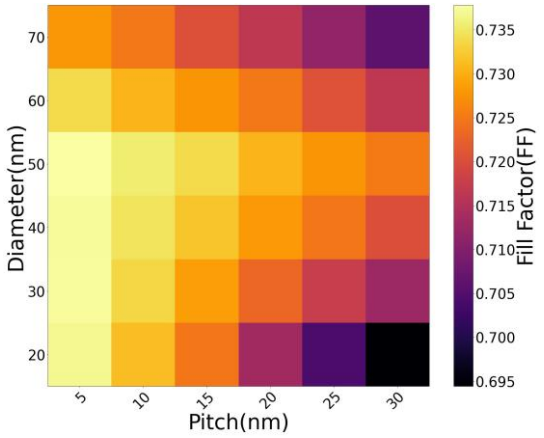

Fig. 7: Variations in Fill Factor (FF) with respect to diameter and pitch of SWCNT nanorods embedded in a Si thin-film solar cell.

nm diameter and pitch size of 5 nm, compared to the output power of 1.624 mW/cm^2 from bare Si substrate. Increasing the pitch size from 10 to 30 nm as mentioned earlier gradually reduces output power values, respectively. Since the maximum output power depends on the J_{SC}, V_{OC}, and fill factor, it follows a trend similar to theirs.

6) Efficiency Analysis: Efficiency reflects the performance of a solar cell and is indicative of the percentage of the incident optical power from the sun that is converted to electrical power (i.e., through the generation of electron-hole pairs), and so is the most common parameter for solar cell analysis. As shown in Fig. 9, the highest efficiency is obtained for nanorods of 30 nm diameter and 5 nm pitch size - 8.504%, compared to the bare Si substrate having 1.624% efficiency. The efficiency decreases to 7.22, 6.55, 5.98, 5.53, and 5.19% as the pitch size is increased to 10, 15, 20, 25, and 30 nm respectively, following a pattern similar to that of output power (P_{max}).

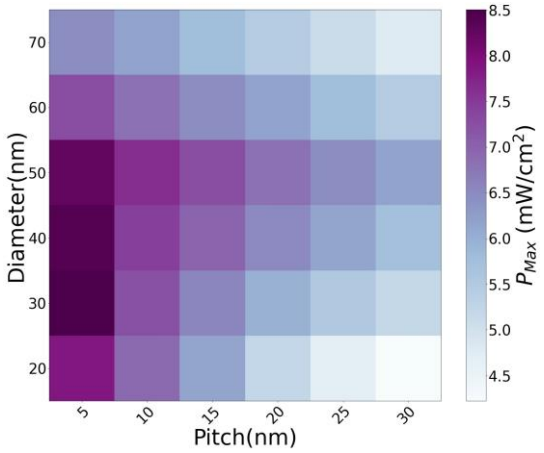

Fig. 8: Variations in maximum output power (P_{max}) with respect to diameter and pitch of SWCNT nanorods embedded in a Si thin-film solar cell.

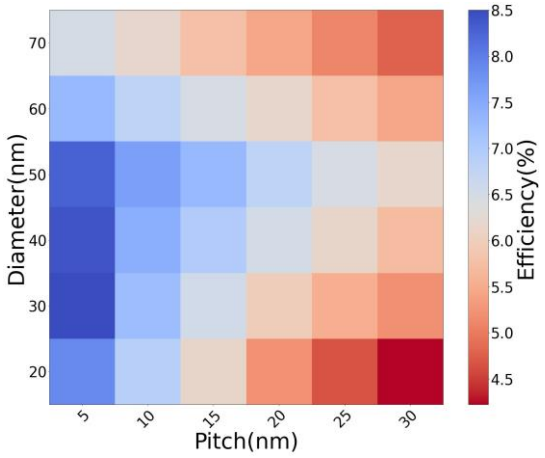

Fig. 9: Variations in % efficiency (η) with respect to diameter and pitch of SWCNT nanorods embedded in a Si thin-film solar cell.

7) Optical Absorption Factor Analysis (g): This is the sum of 150 frequency points across the wavelength range 400 nm-1100 nm range. This parameter indicates how much light is absorbed by the SWCNT nanorod embedded TFSC and also the bare Si TFSC. Like the trends seen in J_{SC}, the value of g starts of as maximum and gradually decreases for all diameters of nanorods, as shown in Fig. 10. The highest value was obtained for a diameter of 30 nm and pitch 5 nm. This lends support to the results obtained for maximum J_{SC} and (P_{max}) for the same configuration as more optical power (e.g., sunlight) is absorbed in the optimal structure. When pitch changes from 5-30 nm for the 30 nm diameter nanorods, the g values varies from 1340.79, 1160.75, 1079.75, 1005.53, 933.51, and 883.3. This progressive decrease in g value can be related to the decreasing trends observed in J_{SC} (see Fig. 5).

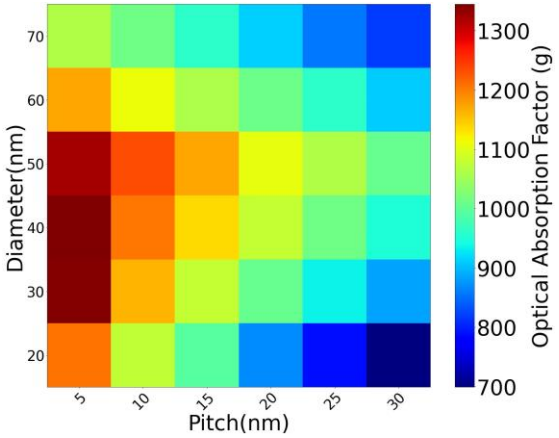

Fig. 10: Variations in the optical absorption factor (g) with respect to diameter and pitch of SWCNT nanorods embedded in a Si thin-film solar cell.

B. Optical Near-Field Analysis

Optical near-field is a graphical representation of the electromagnetic (EM) field distribution in the proximity of SWCNT nanorod(s) embedded in Si TFSC. In Fig.11(a), it is eminent that there is maximum EM field enhancement at the top of the substrate where the SWCNT nanorods are exposed to the air. The hotspots or enhanced EM field zones are followed by low EM fields and then again followed by hotspots, albeit of lower intensity than the top surface layer, thus showing the effects of constructive and destructive interferences. Similarly, enhancement zones can be seen in between the nanorods, indicating scattering of light by the nanorods into the neighboring Si substrate. From Fig.11(b), it can be deduced that light scattered from the two adjacent nanorods constructively interfere and produce stronger EM field zones in the Si substrate than within the nanorods. The optical near-field enhancement plots were computed using procedures discussed previously [4] [20]. Table I shows a direct comparison of the different opto-electronic performance parameters between a bare Si TFSC and the optimal configuration of SWCNT nanorods embedded in a Si TFSC. The data in Table I clearly shows the beneficial effects of embedding SWCNTbased nanorods within the absorbing layer of the solar cell as indicated by the superior opto-electronic performance parameters generated. The optical nearfield enhancement plot further explains why 5 nm pitch of SWCNT-based nanorods result in optimal parameters. As the nanorods are more densely packed, there are stronger plasmon resonance modes interacting with adjacent nanorods, leading to stronger electric fields and hence higher electron-hole pair generation.

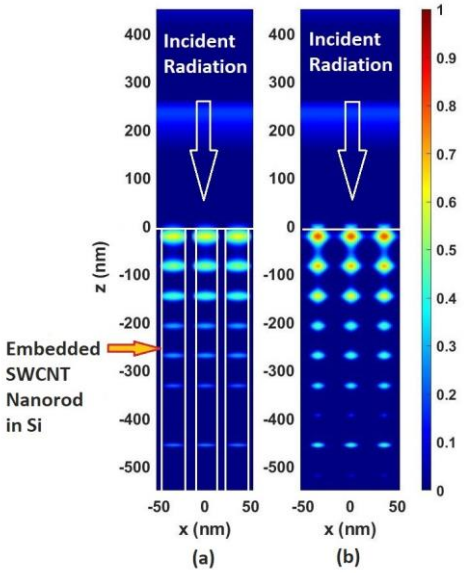

Fig. 11: Enhancements of optical near-field (at λ = 520 nm) for optimal SWCNT nanorod structure for: (a) x-z plane monitor bisecting through a row of nanorods (b) x-z plane monitor placed in between two rows of nanorods.

TABLE I: Comparison of solar cell performance parameters between bare Si TFSC and optimal configuration of SWCNT nanorods embedded in a Si TFSC.

Configuration	J_{SC} (mA/cm^2)	V_{OC} (V)	Fill Factor	P_{max} (mW/cm^2)	Efficiency
Bare Si	7.12	0.31	0.73	1.62	1.62%
Optimized with embedded SWCNT nanorod	32.13	0.36	0.74	8.50	8.50%

IV. Conclusion

This computational study investigates the possibility of using arrays of SWCNT-based nanorods embedded in silicon thin-film solar cells (TFSCs) to enhance the opto-electronic performance of the solar cells (i.e., light absorbed to electric current generation efficiency). The finite-difference timedomain (FDTD) method was used to investigate the effect of varying the diameter of the nanorods and the inter-nanorod spacing (pitch) when embedded within the absorbing layer of a Si TFSC. It was found that such SWCNTs can significantly help to improve the optoelectronic performance levels of Si TFSCs. Several different configurations of SWCNT embedded nanorod structures were investigated and the optimal nano rod structure had a diameter of 30 nm and a side-to-side pitch of 5 nm. This configuration generated a short circuit density of 32.13 mA/cm^2, which was approximately 4-fold larger when compared to that of a bare Si TFSC (J_{SC} for bare Si was 7.124 mA/cm^2). Additionally, such optimal configurations of the SWCNT embedded nanorod structure showed several-fold increase in the efficiency when compared to a bare Si TFSC. The optimal structure was shown to have a broadband optical absorption enhancement compared to that of bare Si substrate (as seen by the large optical absorption factor (g)). Future studies will look into using SWCNT film materials as an electrode material and also investigate the possibility of coupling plasmonic metal nanoparticles in various configurations related to the SWCNT embedded nanorod structure(s) to explore ways to further enhance the opto-electronic performance levels of solar cells.

Acknowledgment

The authors would like to convey their gratitude to Independent University, Bangladesh (IUB) for financing this research (Research Project No: 2021-SETS-08) and provide further logistic support.

References

[1] K. Catchpole and A. Polman, "Plasmonic solar cells," *Optics express*, vol. 16, no. 26, pp. 21793–21800, 2008.

[2] P. Jokic and M. Magno, "Powering smart wearable systems with flexible solar energy harvesting," in *2017 IEEE International symposium on circuits and systems (ISCAS)*. IEEE, 2017, pp. 1–4.

[3] A. Belghachi, "Detailed analysis of surface recombination in crystalline silicon solar cells," in *2013 international renewable and sustainable energy conference (IRSEC)*. IEEE, 2013, pp. 161–166.

[4] A. J. Haque, A. A. Suny, R. B. Sultan, T. A. Khan, and M. H. Chowdhury, "Effects of "defective" plasmonic metal nanoparticle arrays on the opto-electronic performance of thin-film solar cells: computational study," *Applied Optics*, vol. 62, no. 12, pp. 3028–3041, 2023.

[5] F. E. Subhan, A. D. Khan, F. E. Hilal, A. D. Khan, S. D. Khan, R. U. Khan, M. Imran, and M. Noman, "Correction: Efficient broadband light absorption in thin-film a-si solar cell based on double sided hybrid bi-metallic nanogratings," *RSC advances*, vol. 10, no. 29, pp. 16881– 16881, 2020.

[6] W. Chen, J. Tao, H. Xu, D. Gao, J. Lv, Y. Qin, G. Guo, X. Li, Q. Wang, Z. An *et al.*, "Surface silicon nanostructure for enhancement of blue light absorption," *Results in Physics*, vol. 32, p. 105133, 2022.

[7] I. Jeon, Y. Matsuo, and S. Maruyama, "Single-walled carbon nanotubes in solar cells," *Single-Walled Carbon Nanotubes: Preparation, Properties and Applications*, pp. 271–298, 2018.

[8] M. C. Beard, J. L. Blackburn, and M. J. Heben, "Photogenerated free carrier dynamics in metal and semiconductor single-walled carbon nanotube films," *Nano letters*, vol. 8, no. 12, pp. 4238–4242, 2008.

[9] X.-G. Hu, P.-X. Hou, C. Liu, F. Zhang, G. Liu, and H.-M. Cheng, "Small-bundle single-wall carbon nanotubes for high-efficiency silicon heterojunction solar cells," *Nano Energy*, vol. 50, pp. 521–527, 2018.

[10] K.-C. Chiu, A. L. Falk, P.-H. Ho, D. B. Farmer, G. Tulevski, Y.-H. Lee, P. Avouris, and S.-J. Han, "Strong and broadly tunable plasmon resonances in thick films of aligned carbon nanotubes," *Nano letters*, vol. 17, no. 9, pp. 5641–5645, 2017.

[11] M. Fasihbeiki, F. A. Boroumand, A. Khademi, and A. SoleimaniGorgani, "Improving the electrical properties of polymer solar cells using swcnt," in *2014 22nd Iranian Conference on Electrical Engineering (ICEE)*. IEEE, 2014, pp. 338–340.

[12] F. Previti, S. Patane, and M. Allegrini, "Polymer heterostructures with` embedded carbon nanotubes for efficient photovoltaic cells," *Applied surface science*, vol. 255, no. 24, pp. 9877–9879, 2009.

[13] S. Park, M. Vosguerichian, and Z. Bao, "A review of fabrication and applications of carbon nanotube film-based flexible electronics," *Nanoscale*, vol. 5, no. 5, pp. 1727–1752, 2013.

[14] J. Yoon, U. Kim, Y. Yoo, J. Byeon, S.-K. Lee, J.-S. Nam, K. Kim, Q. Zhang, E. I. Kauppinen, S. Maruyama *et al.*, "Foldable perovskite solar cells using carbon nanotube-embedded ultrathin polyimide conductor," *Advanced Science*, vol. 8, no. 7, p. 2004092, 2021.

[15] R. A. Sayer, S. L. Hodson, and T. S. Fisher, "Improved efficiency of dyesensitized solar cells using a vertically aligned carbon nanotube counter electrode," 2010.

[16] A. Abdulhameed, "Carbon nanotube alignment methods," *Carbon Nanotubes-Recent Advances, New Perspectives and Potential Applications*, 2022.

[17] Photonics simulation software — Ansys Lumerical, https://www.ansys.com/products/photonics (accessed July 15, 2023).

[18] G. A. Ermolaev, A. P. Tsapenko, V. S. Volkov, A. S. Anisimov, Y. G. Gladush, and A. G. Nasibulin, "Express determination of thickness and dielectric function of single-walled carbon nanotube films," *Applied Physics Letters*, vol. 116, no. 23, 2020.

[19] C.B.Honsberg and S.G.Bowden, Photovoltaics Education Website, https://www.pveducation.org/ (accessed July 6, 2023).

[20] M. M. Shaky and M. H. Chowdhury, "Bowtie-based plasmonic metal nanoparticle complexes to enhance the opto-electronic performance of thin-film solar cells," *Applied Optics*, vol. 60, no. 17, pp. 5094–5103, 2021.

[21] D. Bandurin, E. Moench, K. Kapralov, I. Phinney, K. Lindner, S. Liu, J. Edgar, I. Dmitriev, P. Jarillo-Herrero, D. Svintsov *et al.*, "Cyclotron resonance overtones and near-field magnetoabsorption via terahertz bernstein modes in graphene," *Nature Physics*, vol. 18, no. 4, pp. 462– 467, 2022.

[22] C. Li, Y. Chen, Y. Wang, Z. Iqbal, M. Chhowalla, and S. Mitra, "A fullerene–single wall carbon nanotube complex for polymer bulk heterojunction photovoltaic cells," *Journal of Materials Chemistry*, vol. 17, no. 23, pp. 2406–2411, 2007.